DOI: 10.1002/ejic.200700040

Electronic Structure of Linearly Coordinated EQ Complexes of the Type [$(N_3N)W(EQ)$] [$N_3N = N(CH_2CH_2NSiMe_3)_3$; E = P, As, Sb, Bi; Q = O, S, Se, Te]: A DFT Study

Gábor Balázs,[a] Jennifer C. Green,*[a] and D. Michael P. Mingos*[b]

Keywords: Bonding / Pnicogens / Chalcogens / Tungsten / Density functional calculations

Density functional theory (DFT) calculations were carried out on the terminal EQ complexes [$(N_3N)W(EQ)$] {$N_3N = N(CH_2CH_2NSiMe_3)_3$; E = P, As, Sb, Bi; Q = O, S, Se Te} to clarify the bonding situation within the linear N_{ax}–W–E–Q core. This unusual structural motif gives rise to a bonding arrangement in which the π-electron density is delocalised over the three atoms of the W–E–Q unit. Fragment calculations and natural bond order (NBO) data indicated that the σ-bonding component of the N_{ax}–W–E–Q unit comprises two occupied σ orbitals, while the π component of bonding comprises two sets of degenerate π orbitals. In general, the π orbitals of the N_{ax}–W–E–Q core are higher in energy compared to the σ orbitals. The phosphorus monoxide (EQ = PO) complexes provide an exception to this rule, with the 1π orbitals of the W–P–O core lower in energy than the σ orbitals. Generally, as the atomic number of either the pnicogen (E) or chalcogen (Q) atom increases the extent of σ-orbital delocalisation decreases, whereas the π-orbital delocalisation increases. Fractional bond orders and Wiberg bond indices were used to establish whether localisation of the π-electron density gives rise to a W–E or an E–Q double or triple bond. Both methods indicate a W–E as well as an E–Q double bond. The ionic nature of the complexes were analysed by inspection of the Hirschfeld charge distribution which shows only a moderate ionic character. Exceptions are the pnicogen monoxide complexes, which are more ionic.

Introduction

Transition metal complexes of nitrogen monoxide (NO) underwent significant research in the early 1970s as a result of the wide range of bonding motifs that can be adopted by this versatile ligand. NO represented the fore-runner of a wider range of the pnicogen–chalcogen (E–Q) moieties bonding to a variety of transition metal fragments.[1] The coordination chemistries of the heavier EQ analogues (E = P, As, Sb, Bi; Q = O, S, Se, Te) remain relatively poorly studied. This is partly due to the unavailability of the free EQ ligands as well as to their poor coordinating abilities.[2] The majority of transition metal complexes bearing heavier EQ ligands contain PQ (Q = O, S, Se and Te) ligands that are coordinated to three metal centres in a μ_3 fashion. Selected examples include [$\{Ni(C_5iPr_4H)\}_2W(CO)_4(\mu_3\text{-}PO)_2$],[3] [$\{Ru(CO)\}_3(\mu_3\text{-}PO)]^-[iPr_2NH_2]^+$[4] [$\{W(CO)_2Cp\}_3(\mu_3\text{-}PS)$],[5] [$\{Co(C_5tBu_2H_3)\}_3(\mu_3\text{-}PQ)_2$] (Q = O, S, Se),[6] [$\{Co(C_5tBu_2H_3)\}_3(\mu_3\text{-}PQ)(\mu_3\text{-}P)$] (Q = Se,[5] Te[6]), [$\{Ni(C_5iPr_4H)\}_2W(CO)_4(\mu_3\text{-}PS)_2$][7] and [$\{FeCp(CO)_2\}\{Fe_2(CO)_3Cp_2\}(\mu_3\text{-}PS)_2$].[8] The synthesis of such PQ-containing complexes is typically achieved by oxidation of the corresponding phosphido complex with the chalcogen (e.g. S, Se, Te) or a suitable chalcogen source (e.g. dimethyldioxirane, ethylene sulfide). Hydrolysis of a μ_3-$P(NiPr_2)$ functional group has also been effective in preparation of the more polar PO complex [$\{Ru(CO)\}_3(\mu_3\text{-}PO)]^-[iPr_2NH_2]^+$.[4]

Synthesis of the terminal pnictido complexes [$(ArRN)_3Mo{\equiv}P$] [Ar = 3,5-$Me_2C_6H_3$, R = $C(CD_3)_2Me$][9] and [$(N_3N)W{\equiv}E$] [$N_3N{=}N(CH_2CH_2NSiMe_3)_3$; E = P,[10] As[11,12] and Sb[13]] presented clear opportunities for the preparation of transition metal complexes containing an η^1-coordinated EQ ligands. Indeed, Cummins et al. reported the isolation and characterisation of the PO [$(ArRN)_3Mo(PO)$][14] and PS [$(ArRN)_3Mo(PS)$][9,15] complexes, which were prepared by oxidation of the corresponding phosphido complex [$(ArRN)_3Mo{\equiv}P$] with dimethyldioxirane and sulfur, respectively. More recently, Scheer et al. reported preparation of the η^1-coordinated PS and AsS complexes [$(N_3N)W(ES)$] (E = P and As)[16] by oxidation of the terminal phosphido and arsenido complexes [$(N_3N)W{\equiv}E$] (E = P and As) with cyclohexene sulfide.

The bonding in the η^1-coordinated PS complexes was investigated by Frenking and Wagener who performed calculations on a series of model complexes of the type [$(NH_2)_3M(PS)$] and [$NH_3(NH_2)_3M(PS)$] (M = Mo, W). They proposed two Lewis formulae, one based on an NBO partitioning Scheme (**I**) and a second one based on Wiberg

[a] Inorganic Chemistry Laboratory, Oxford University, South Parks Road, Oxford, OX1 3QR, United Kingdom
[b] St. Edmund Hall, Oxford University, Queen's Lane, Oxford OX1 4AR, UK
E-mail: jennifer.green@chem.ox.ac.uk
Supporting information for this article is available on the WWW under http://www.eurjic.org or from the author.

bond indices (**II**). Both resonance canonical forms represented as Lewis structures are depicted in Scheme 1.[18] The dissociation of an amido ligand from the metal atom in **II** makes that Lewis structure less likely. The electron count of complexes of the type $[NH_3(NH_2)_3M(EQ)]$ depend on whether the amido nitrogen atoms are one- or three-electron donors. Since the a_2 combination of the lone-pair orbitals of the three amido ligands does not have a symmetry match among the tungsten orbitals (the three amido nitrogen atoms effectively donate seven electrons altogether), it follows that complexes of the type $[NH_3(NH_2)_3M(EQ)]$ obey the 18-electron rule, and the complexes of the type $[(NH_2)_3M(PS)]$ are 16-electron species.

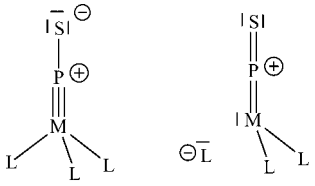

Scheme 1. Proposed Lewis structures of $[L_nM(PS)]$ complexes.[17]

Recently, we reported the results of calculations on $[(N_3N)W(ES)]$ $[N_3N=N(CH_2CH_2NSiMe_3)_3$; E = P, As and Sb].[16] Inclusion of the Me_3Si substituents on the imido nitrogen atoms was important for achieving good agreement of our calculated geometries with structural parameters obtained from X-ray crystallographic analyses of these complexes. We assume this is due to the strong electron-donating properties of these substituents. Most significantly, our study demonstrated that π bonding in the W–E–Q unit can best be described as two three-centre four-electron bonds (3c-4e).[16] To further our understanding of the structural and electronic properties of η^1-coordinated EQ complexes, we have extended our analysis to the complete series of $[(N_3N)W(EQ)]$ complexes (E = P, As, Sb, Bi; Q = O, S, Se and Te). In this paper we analyse the structural trends and use several theoretical tools to gain insight into the important bonding features for the heavier EQ ligands.

Results and Discussion

Geometries and Binding Energies

Calculated geometries for complexes **1**–**4** were pseudo-C_3-symmetric with the N_{ax}–W–E–Q core aligned with the C_3 axis. Given the isostructural nature of these complexes, the optimised geometry of $[(N_3N)W(PO)]$ (**1a**) is depicted in Figure 1 as representative of this series. Selected bond lengths and angles for the calculated structures are provided in Table 1. Our benchmarks for the optimised structures are the complexes **1b** and **2b**, whose crystal structures were reported recently.[16] The calculated geometrical parameters for **1b** (P–S 1.94 Å; W–P 2.15 Å) and **2b** (As–S 2.05 Å; W–As 2.25 Å) compare excellently with the reported experimental values [E–S 1.9410(16) Å and 2.048(2) Å; W–E 2.1579(10) Å and 2.2557(8) Å for **1b** and **2b**, respectively].[16] The N_{ax}–W distances in **1b** (2.22 Å) and **2b** (2.21 Å) also agree favourably with the reported experimental values for these complexes [**1b** 2.217(3) Å; **2b** 2.214(6) Å].[16] Earlier calculations on the pnictido complexes $[(N_3N)W{\equiv}E]$ (E = P, As, Sb and Bi)[12,13] provided N_{ax}–W distances that were longer than those measured in single-crystal X-ray analysis of these complexes.

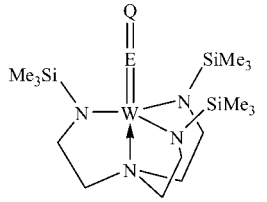

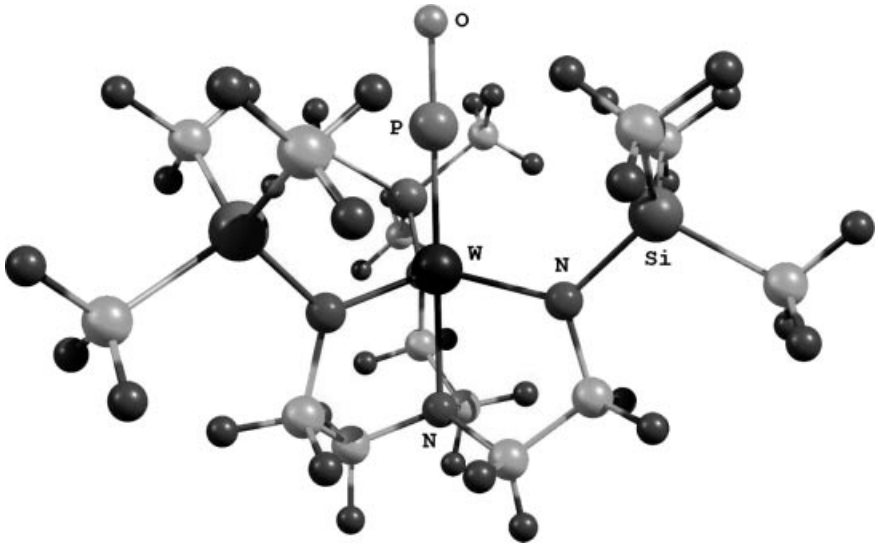

Figure 1. Calculated geometry of $[(N_3N)W(PO)]$ (**1a**).

Table 1. Calculated bond lengths [Å] and W–E and E–Q bond dissociation energies (BDE). The experimental bond lengths for **1b** and **2b** are given in parentheses.

	E	Q	E–Q	W–E	N_{ax}–W	N_{eq}–W (av.)	W–E BDE [kJ/mol]	E–Q BDE [kJ/mol]
1a	P	O	1.48	2.13	2.21	1.995	–414.6	–557.6
1b		S	1.94 (1.940)	2.15 (2.158)	2.22 (2.217)	1.98 (1.99)	–400.9	–348.8
1c		Se	2.08	2.15	2.23	1.98	–399.6	–286.6
1d		Te	2.30	2.16	2.23	1.98	–401.0	–211.9
2a	As	O	1.64	2.24	2.20	1.99	–340.9	–438.5
2b		S	2.05 (2.048)	2.25 (2.256)	2.21 (2.214)	1.98 (1.99)	–338.9	–301.6
2c		Se	2.18	2.25	2.22	1.98	–339.4	–255.3
2d		Te	2.39	2.26	2.22	1.98	–340.2	–196.5
3a	Sb	O	1.84	2.44	2.19	1.99	–259.1	–382.9
3b		S	2.25	2.45	2.20	1.98	–262.4	–280.6
3c		Se	2.36	2.46	2.20	1.98	–258.9	–244.3
3d		Te	2.58	2.46	2.21	1.98	–261.3	–189.5
4a	Bi	O	1.94	2.53	2.19	1.99	–203.7	–326.1
4b		S	2.34	2.53	2.19	1.99	–206.8	–248.4
4c		Se	2.46	2.54	2.19	1.99	–205.4	–218.7
4d		Te	2.662	2.54	2.19	1.99	–207.6	–172.6

The experimental N_{ax}–W distances in pnictido complexes [$(N_3N)W{\equiv}E$] [2.34(1) Å, 2.336(6) Å and 2.33(1) Å for E = P,[10] As[12] and Sb,[13] respectively] are longer than in the complexes **1**–**4**, showing the stronger *trans* influence of an E ligand compared to an EQ ligand. Although the variation of the N_{ax}–W distance with the nature of the EQ ligand is small a trend can clearly be observed. In general, the N_{ax}–W distance decreases as the atomic number of E increases, indicating that EQ ligands of the heavier pnicogens exhibit a weaker *trans* influence than their lighter analogues (Figure 2). In contrast, as the atomic number of Q increases the N_{ax}–W distance increases, indicating that EQ ligands of the heavier chalcogens exhibit a stronger *trans* influence.

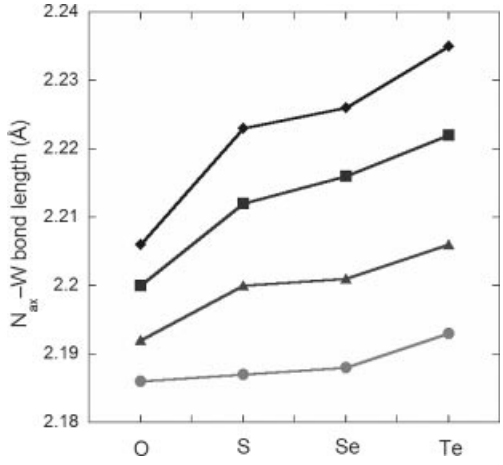

Figure 2. Variation of the N_{ax}–W distances [Å] with Q in complexes [$(N_3N)W(EQ)$] (**1**–**4**). Legend: P = ♦, As = ■, Sb = ▲ and Bi = ●.

The major differences in the structure upon moving from the lighter to the heavier congeners is observed in the W–E and E–Q distances. As expected, as the atomic number of E or Q increases, the E–Q and the W–E bond lengths also increase. The shortest E–Q distance is predicted for **1a** (1.48 Å) and the longest distance for **4d** (2.66 Å). The W–E distance increases only slightly for a particular E, as Q becomes heavier (Figure 3). This trend is observed when E = P, As and Sb, whereas for the BiQ complexes the W–Bi distance remains constant on going from Q = O to Te.

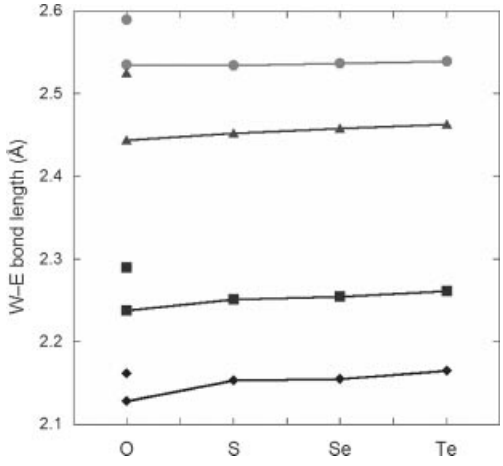

Figure 3. Variation of the W–E distances in complexes [(N_3N)-W(EQ)] (**1**–**4**). Legend: P = ♦, As = ■, Sb = ▲ and Bi = ●. The detached points correspond to the experimental W–E distances in the corresponding [$(N_3N)W{\equiv}E$] complexes for E = P, As and Sb and with the calculated distance for E = Bi.

Comparison of the W–E distances in the complexes **1**–**4** with the experimental W–E distances in the pnictido complexes [$(N_3N)W{\equiv}E$] (E = P, As, and Sb) [2.162(4) Å,[10] 2.2903(11) Å[12] and 2.5255(17) Å[13] for E = P, As and Sb, respectively] shows that, upon oxidation of the [(N_3N)-$W{\equiv}E$] complexes, the W–E distance became shorter, a phenomenon which is more accentuated for the heavier homologues of E (Figure 3). The exception is the phosphorus monotelluride complex **1d** in which the predicted W–P dis-

tance is slightly longer than the W–P distance in the corresponding phosphido complex. A similar shortening is observed for the experimental Mo–P distance in [$(ArRN)_3$-Mo(PQ)] (Q = O,[14] S[15]) where the Mo–P distances are 0.04 Å and 0.09 Å shorter than in the parent pnictido complex [$(ArRN)_3Mo{\equiv}P$].[9] The W–E distances in complexes **2**–**4** are comparable to the sum of the triple-bond covalent radii[19] of the corresponding elements, whereas in complexes **1** the W–E distances are slightly longer.

In order to gain insight into the strength of the E–Q bonding and stability of the complexes, the E–Q bond dissociation energies were calculated (Table 1). This shows that complexes **1**–**4** are stable with respect to the dissociation into the pnictido complexes and chalcogen. Furthermore, the E–Q bond dissociation energies present the expected periodic variation; an approximately linear decrease for a given pnicogen (E) upon going from Q = S to Te (Figure 4). The pnicogen monoxide complexes (**a**) exhibit a larger BDE than would be anticipated upon linear extrapolation of the BDE plots for complexes **b**–**d**. The stability of the complexes is also supported by the high HOMO–LUMO gap.

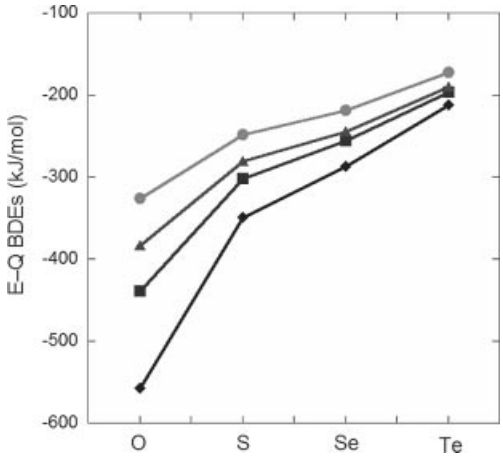

Figure 4. Variation of the E–Q bond dissociation energies [kJ/mol] in complexes [$(N_3N)W(EQ)$] (**1**–**4**). Legend: P = ♦, As = ■, Sb = ▲ and Bi = ●.

The E–Q BDEs also demonstrate a dependence on the atomic number of the pnicogen (E) for a given chalcogen (Q). For example, complexes **a** (Q = O), show a decrease in the BDE going from **1a** to **4a**.

To enable the comparison of the strength of the W–E bonding in the complexes **1**–**4** with the parent pnictido [$(N_3N)W{\equiv}E$] complexes, the W–E BDEs were calculated. Similarly to the E–Q BDEs, the W–E BDEs decrease as the atomic number of E increases for a particular Q, but are not influenced by the nature of Q (Table 1). The comparison of the W–E BDEs in complexes **1**–**4** (Table 1) and the pnictido complexes [$(N_3N)W{\equiv}E$] (481.9 kJ/mol, 429.0 kJ/mol, 333.4 kJ/mol and 293.3 kJ/mol for E = P, As, Sb and Bi, respectively)[13] shows that the strength of the W–E bonding is ca. 80–100 kJ/mol weaker in the complexes **1**–**4** than in the parent pnictido complexes. This shows that upon oxidation of the pnictido complexes the W–E triple bond is weakened thermodynamically.

Bonding Analysis

The bonding arrangement in complexes **1**–**4** was further probed using fragment calculations and Natural Bond Orbital (NBO) analyses. Complexes **1**–**4** were separated into two fragments either by cleavage of the E–Q bond, to provide (N_3N)WE and Q fragments, or by cleavage of the W–E bond to provide (N_3N)W and EQ fragments. Contributions to the bonding in the [$(N_3N)W(EQ)$] complex can then be understood in terms of linear combinations of the fragment MOs. The bonding in the complex [(N_3N)W-

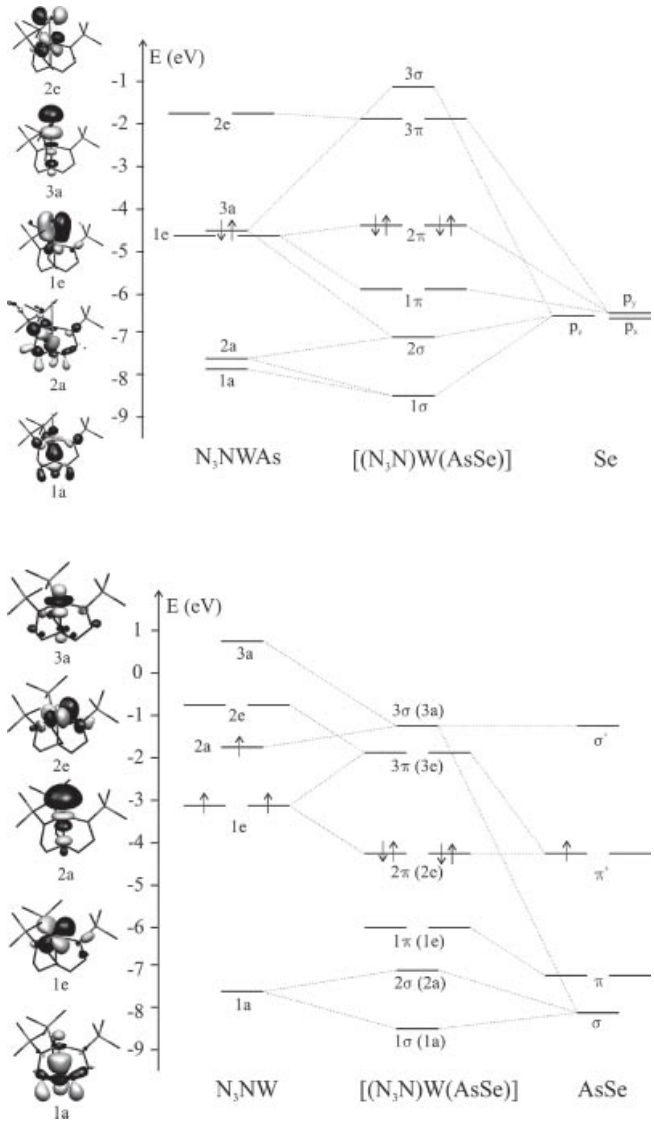

Figure 5. Molecular orbital interaction scheme for [$(N_3N)W(AsSe)$] (**2c**). The (N_3N)W and (N_3N)WAs fragment levels are labelled in C_3 symmetry and those of **2c** with σ and π symmetry with respect to the NWAs axis (the labels in parentheses are in C_3 symmetry). The relevant molecular orbitals of the (N_3N)W and (N_3N)WAs fragments are given on the left-hand side of the diagram.

(AsS)] (**2b**) was described elsewhere.[16] Here we describe the bonding in the complex [(N3N)W(AsSe)] (**2c**) as a representative example of this series of structures in order to give a basis for discussion of the trends in the bonding upon moving from the lighter EQ congeners to the heavier ones.

The molecular orbital interaction scheme for the complex **2c** is depicted in Figure 5. The (N3N)W and (N3N)WAs fragment levels are labelled in C_3 symmetry and those of the complex with σ and π symmetry (the labels in the C_3 symmetry are given in parentheses) with respect to the NWAs axis. The relevant molecular orbitals of the (N3N)W and (N3N)WAs fragments are given on the left-hand side of the diagram.

The results of a fragment analysis, in which the complex **2c** was separated into an Se and an (N3N)WAs fragment, shows that the p_z orbital of Se mixes with the 1a orbitals of the (N3N)WAs fragment, containing contributions from N_{ax} (p_z), As (p_z) and W (d_{z^2} and s) to form two occupied molecular orbitals of σ symmetry (1σ and 2σ, Figures 5 and 6). 1σ is an all-in-phase combination, whereas 2σ is As–Se bonding, but has minimal W contribution and thus is W–As and W–N_{ax} nonbonding. The p_x and p_y orbitals of the Se interact with the two degenerate π orbitals of the WAs unit (1e) to give two occupied sets of π orbitals (1π and 2π) from which the 1π set is bonding over all three atoms (W, As and Se) but with only a minor contribution from W. The 2π set is antibonding with respect to the AsSe and bonding with respect to the WAs unit (Figure 6).

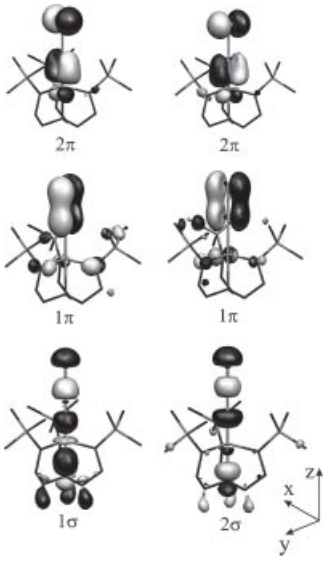

Figure 6. Isosurfaces of 2π (2e), 1π (1e) and 1σ (1a) and 2σ (2a) MO of [(N3N)W(AsSe)] (**2c**).

An analysis of the interaction of the AsSe fragment with the (N3N)W fragment shows that the π orbitals of the AsSe fragment increase slightly in energy due to the increasing charge, but do not mix significantly with the orbitals of the (N3N)W fragment, remaining localised as As–Se π bonds (forming 1π in the complex; Figures 5 and 6). In contrast, the π* orbitals of the AsSe fragment interact with the orbitals 1e of the (N3N)W fragment, containing mainly the tungsten d_{yz} and d_{xz} orbitals, respectively, to give a W–As π-bonding interaction (2π). The out-of-phase combination is unoccupied and forms the LUMO (3π). The 2π MO encapsulates back-donation of the tungsten atom to the AsSe ligand. Overall, the WAsSe π system is best described by two three-centre four-electron (3c-4e) bonds. This orbital interaction scheme describes qualitatively the bonding in complexes **1**–**4**.

General Trends

Although the bonding in complexes **1**–**4** is similar, significant changes appear in the σ bonding going from the lighter to the heavier homologues. In the pnicogen monoxide complexes (**1a**–**4a**) the contribution of atomic orbitals of E to 1σ decreases as its atomic number increases (Figure 7). However, the most distinct changes were observed for the pnicogen monotelluride complexes **1d**–**4d** (Figure 8). In the PTe complex (**1d**) the 1σ is an extended bonding MO over the N_{ax}–W–E–Q core. In contrast to that the 1σ in the bismuth monotelluride complex (**4d**) is a localised N_{ax}–W bonding molecular orbital, having a strong 1a contribution

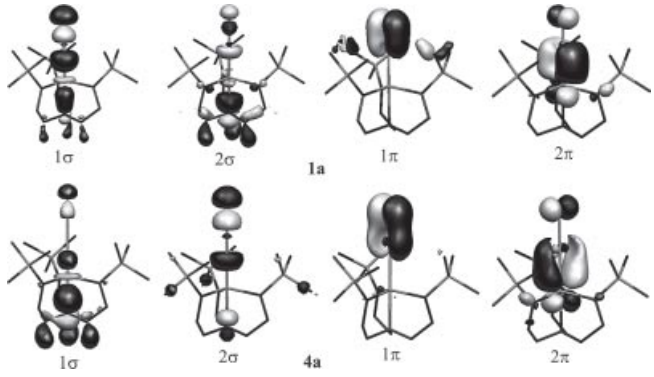

Figure 7. Isosurfaces of the 1σ, 2σ, 1π and 2π MOs of the phosphorus monoxide and bismuth monoxide complexes **1a** and **4a**, respectively. From the degenerated 1π and 2π sets only one orbital is represented.

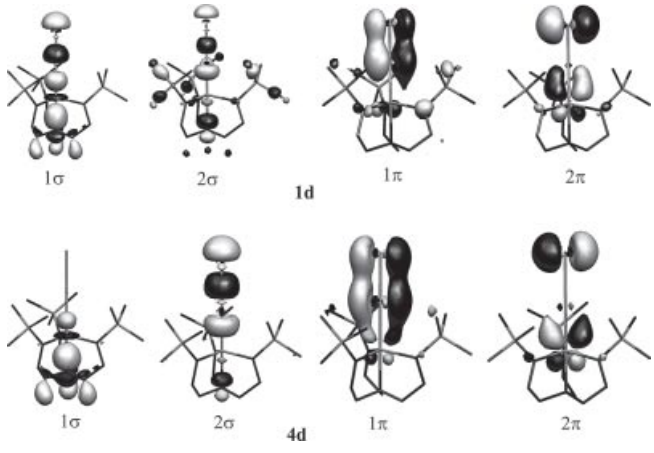

Figure 8. Isosurfaces of the 1σ, 2σ, 1π and 2π MOs of the phosphorus monotelluride complexes **1d** and **4d**, respectively. From the degenerate 1π and 2π sets only one orbital is represented.

(88.2%) of the N_3NW fragment. The bonding in the arsenic and antimony montelluride complexes (**2d** and **3d**, respectively) constitute a transition between the two extremes (**1d** and **4d**). In **2d** and **3d** there is a mixing of the ETe (E = As, Sb) fragment σ orbital with $(N_3N)W$ fragment orbitals containing Si and C p-orbital contributions. A comparative energy level diagram is given in Figure 9. For 2σ the opposite trend than for 1σ was observed, but the changes are not so accentuated. Generally, as the atomic number of E increases, its contribution to 2σ increases. Also, the contribution of the EQ fragment σ orbital to 2σ increases as the atomic number of either E or Q increases. This leads to a localised E–Q bonding MO.

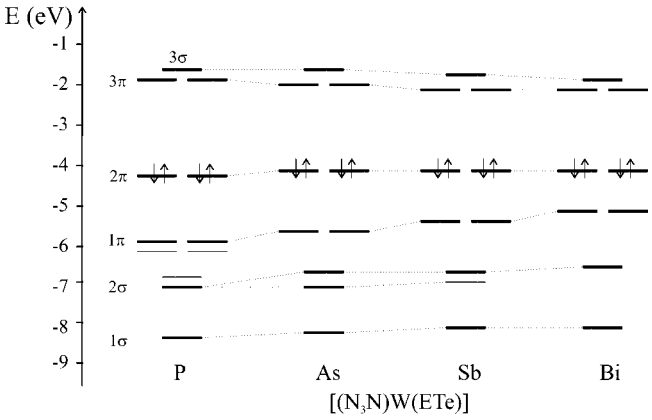

Figure 9. Comparative MO energy level diagram for the pnictido monotelluride complexes $[(N_3N)W(ETe)]$ (**1d**–**4d**). The energy levels marked with thin lines ("ghost" levels) represent combinations of the ETe fragment σ or π orbitals with energetically close-lying orbitals of the $(N_3N)W$ fragment localised on the N_3N ligand. The contribution of the ETe fragment orbitals to the "ghost" levels is relatively small, except for E = As.

The nature of the 1σ MO can explain the relative strength of the *trans* influence of the EQ ligands. The complexes with an extended 1σ MO over the N_{ax}–W–E–Q core, such as the phosphorus monotelluride complex (**1d**) have a stronger *trans* influence than the complexes with 1σ localised on N_{ax}–W (Figures 2 and 8). However, the *trans* influence of the EQ ligands in complexes **1**–**4** (Figure 2) can easily be rationalised in terms of the interaction of the $(N_3N)W$ and EQ fragments σ-type orbitals. The stronger the interaction of the EQ σ orbital with the 1a orbital of the $(N_3N)W$ fragment (Figure 5) the weaker the N_{ax}–W orbital interaction. Since the energy of the 1a orbital of the relaxed $(N_3N)W$ fragment does not change, the *trans* influence will be determined by the relative energy of the EQ fragment σ orbitals. For example, in the case of the PQ complexes (**1**) the energy difference between the σ orbital of the PQ fragments varies strongly between the PO and PTe (ΔE = 1.793 eV), leading to a variation in the mixing with the $(N_3N)W$ fragment 1a orbital. This variation affects strongly the N_{ax}–W distances and hence leads to a variation in the *trans* influence of the different PQ ligands. In contrast, in the BiQ complexes (**4**) the σ orbitals of the BiQ fragments lie energetically close to each other (overall variation in energy ΔE = 0.616 eV) and therefore the variation in the *trans* influence of the BiQ ligands is much lower.

The analysis of the π bonding in the pnicogen monoxide complexes **1a**–**4a** (Figure 10) shows that the relative energy of the 1π set increases considerably as the atomic number of E increases, whereas the 2π set increases and the 3π set decreases only slightly in energy. The more pronounced increase in the energy of the 1π set going from E = P to As (**1a** to **2a**) is not unexpected if we consider that it contains a higher contribution of the EO fragment π orbitals (69.2, 73.8, 86.8 and 86.7% for E = P, As, Sb and Bi, respectively), as well as a high energy difference of the PO and EO (E = As, Sb and Bi) fragments π orbitals. The consequence of the low energy of the PO fragment π orbital is that in the phosphorus monoxide complex (**1a**) the 1π set is lower in energy than 2σ. A similar orbital energy ordering as for **1a** was reported by Carty et al. for the model complex $[(H_2N)_3Mo(PO)]$.[20] In the EQ complexes **b**, **c** and **d** a similar increase in energy of 1π and 2π set and a decrease in energy of 3π set occurs upon increasing the atomic number of E.

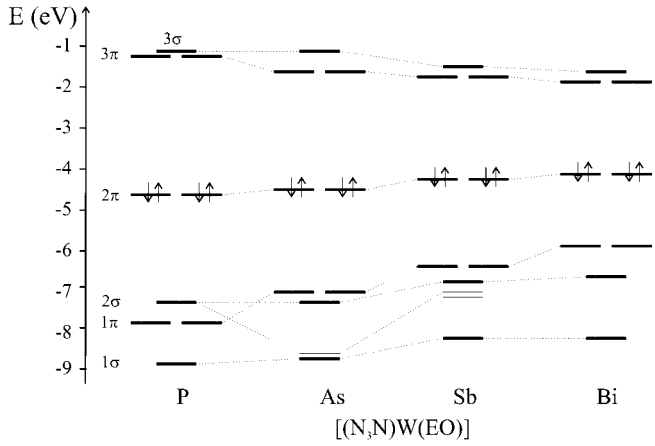

Figure 10. Comparative MO energy level diagram for the pnicogen monoxide complexes $[(N_3N)W(EO)]$ (**1a**–**4a**). The energy levels marked with thin lines ("ghost" levels) represent combination of the EO fragment σ orbitals with energetically close-lying orbitals of the $(N_3N)W$ fragment localised on the N_3N ligand. The contribution of the EO fragment orbitals to the "ghost" levels is relatively small.

Apart from the changes in the energy of the 1π set upon increasing the atomic number of E or Q, changes in the extent of its delocalisation are also apparent. The delocalisation is more accentuated for the heavier congeners (Figures 7 and 8). As the atomic number of the pnicogen E increases, the contribution of the $(N_3N)W$ fragment (1e orbital of the fragment) to the 1π set also increases. Since the 1π set is an in-phase combination over all three atoms (W, E and Q), that leads to a stronger delocalisation of 1π. It is noteworthy, that in phosphorus monotelluride complex **1d** the π set of the PTe fragment mixes not only with the 1e set of the N_3NW fragment to give the 1π set, but also mixes slightly with other orbitals of the N_3NW fragment (containing mainly C, H and Si contributions). That mixing decreases as E becomes heavier so that in the arsenic monotel-

luride complex **2d** only the 1π set contains considerable AsTe π contribution. Changes appears also in the 2π set, which represents the back-bonding of tungsten to the EQ ligand moving from the lighter to the heavier congeners. As the atomic number of E increases, its contribution to the 2π set decreases. That has the effect that 2π becomes permanently weaker bonding (Figure 8). The nature of Q has a similar effect to the nature of E on the 1π and 2π set MOs. Overall, the changes in the π bonding in the complexes **1**–**4** are similar to those in the σ-bonding mainfold; however, they progress in opposite directions.

Based on the fragment calculations we have determined the overall W–E fractional bond order by considering the (N_3N)WE fragment 1e orbitals as W–E bonding, the 2e as W–E antibonding and the 3a orbital as bonding and considering the fragment occupation in the molecule. Similarly, the E–Q fractional bond order can be calculated by considering the occupation of the π, π*, σ and σ* orbitals of the EQ fragment in the complex. Furthermore, by considering the occupations of the fragment σ-type orbitals or π-type orbitals the fractional bond order can be split into a σ- and a π-contribution term. The W–E and E–Q fractional bond orders as well as its σ and π components are summarised in Table 2.

Table 2. Fractional W–E and E–Q bond orders in complexes $[(N_3N)W(EQ)]$ (**1**–**4**).

	E	W–E	E–Q	W–E		E–Q	
				σ	π	σ	π
				Q = O			
1a	P	2.12	2.07	0.35	1.77	0.88	1.19
2a	As	2.09	1.97	0.34	1.75	0.92	1.05
3a	Sb	2.12	2.13	0.34	1.79	0.82	1.31
4a	Bi	2.14	2.18	0.35	1.79	0.87	1.31
				Q = S			
1b	P	2.22	2.03	0.50	1.73	0.86	1.17
2b	As	2.24	1.83	0.49	1.75	0.84	0.99
3b	Sb	2.20	2.12	0.46	1.74	0.83	1.29
4b	Bi	2.23	2.10	0.47	1.76	0.88	1.22
				Q = Se			
1c	P	2.24	1.98	0.52	1.72	0.87	1.11
2c	As	2.26	1.82	0.50	1.76	0.84	0.98
3c	Sb	2.23	2.09	0.48	1.75	0.84	1.25
4c	Bi	2.26	2.08	0.50	1.76	0.89	1.19
				Q = Te			
1d	P	2.32	1.92	0.59	1.73	0.81	1.11
2d	As	2.33	1.73	0.58	1.75	0.74	0.97
3d	Sb	2.28	2.05	0.55	1.73	0.84	1.21
4d	Bi	2.30	2.06	0.56	1.74	0.88	1.18

From Table 2 it may be seen, that the W–E fractional bond orders are lower for the pnicogen monoxide complexes (**1a**–**4a**) than for the complexes of the **b**, **c** or **d** series. For a particular Q the W–E fractional bond order can be considered to be constant within the standard errors. However, as the atomic number of Q increases, for a particular E the fractional bond order increases slightly (Figure 11). The E–Q fractional bond orders do not vary strongly between the complexes **1**–**4**. They increase slightly for a particular Q on going from P to Bi, this being in accordance with the decrease of the tungsten back-donation to the EQ ligand. For a particular E the E–Q fractional bond order decreases on going from O to Te (Figure 12). It is noteworthy that the As–Q fractional bond orders are generally lower, for which the low oxidation ability of As is responsible.

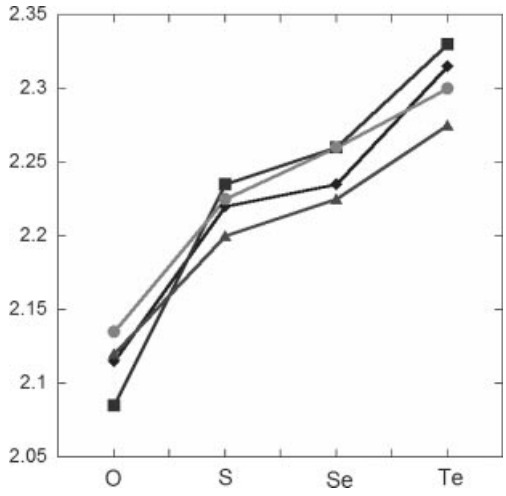

Figure 11. Variation of the W–E fractional bond orders with Q in complexes $[(N_3N)W(EQ)]$ (**1**–**4**). Legend: P = ♦, As = ■, Sb = ▲ and Bi = ●.

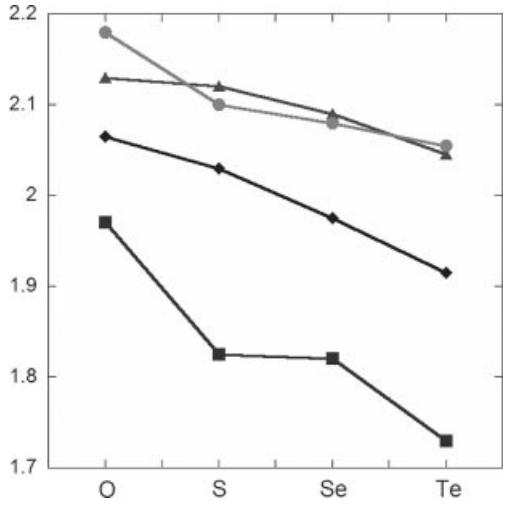

Figure 12. Variation of the E–Q fractional bond orders in complexes $[(N_3N)W(EQ)]$ (**1**–**4**). Legend: P = ♦, As = ■, Sb = ▲ and Bi = ●.

To determine whether the σ and π components of the W–E bond order go in opposite directions, and to obtain insight into the strengths of the σ- and π-bonding ratio, the fractional bond orders were split into their σ and π components (Table 2). The inspection of the σ contributions to the bond orders reveals that the σ part is responsible for the low W–E bond order in the phosphorus monoxide complexes **1a**–**4a**. This increases slightly for a particular E by going from O to Te (Figure 13), while for a particular Q (Q = S, Se and Te) it decreases slightly as the atomic number of E increases. In the pnictido monoxide complexes

the σ component of the W–E fractional bond order stays approximately constant as the atomic number of E increases.

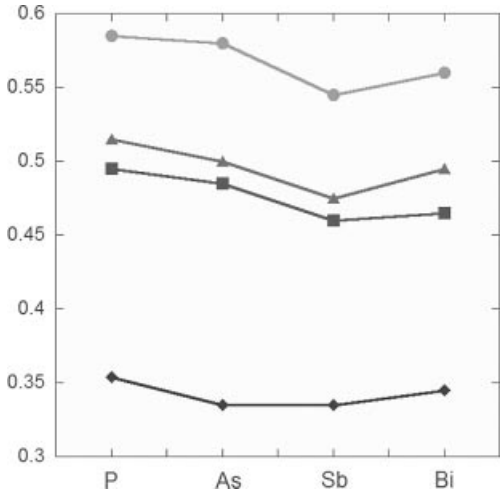

Figure 13. Variation of the σ component of the W–E fractional bond order with E in complexes [$(N_3N)W(EQ)$] (**1**–**4**). Legend: O = ♦, S = ■, Se = ▲ and Te = ●.

The π components of the W–E fractional bond order are not affected by the nature of Q for a particular E and stay essentially constant. Instead, for a particular Q the W–E fractional bond order increases slightly moving from P to Bi. The σ component of the E–Q, as judged by the fractional bond order, is not influenced by either the nature of E or Q, remaining constant. In contrast, the π component of the E–Q bond shows a decrease for a particular E as the atomic number of Q increases and an increase for a particular Q as the atomic number of E increases (Figure 14). The π component of the As–Q fractional bond orders are lower compared with the other complexes, confirming the lower oxidising ability of the arsenic.

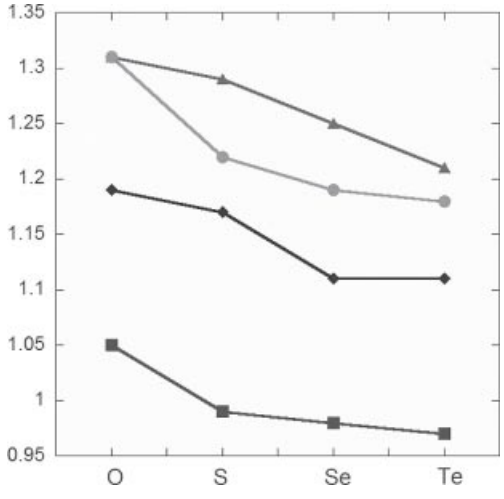

Figure 14. Variation of the π component of the E–Q fractional bond order with Q in complexes [$(N_3N)W(EQ)$] (**1**–**4**). Legend: P = ♦, As = ■, Sb = ▲ and Bi = ●.

The relative small variation of the fractional bond orders does not indicate that the bond strength stays constant. The strength of the bonding or antibonding of the molecular orbitals is not explicitly incorporated in this model and as shown in Table 1 the bond strengths decrease with atomic number.

The relative composition of the σ and π components to the fractional bond order was also investigated. The W–E and the E–Q bonds show a very different σ and π composition. Whereas in the W–E bond σ/π ratio (ca. 1:5 for the EQ complexes and 1:3.6 for the complexes of the series **b**, **c** and **d**) is relatively low, the σ/π ratio of the E–Q bond is much higher (1:1.4).

To enable the comparison of the results obtained with the literature data, we have calculated the Wiberg bond indices (WBI)[21] for the W–E and E–Q bonds of the complexes **1**–**4** (Table 3). Generally, the WBI either of the W–E and E–Q bonds are lower than the corresponding fractional bond orders, but that is compensated by adding a W–Q bond index of which the magnitude varies between 0.3 and 0.4. Similar WBIs were reported for [$NH_3(NH_2)_3W(PS)$] (W–P 1.89 and P–S 1.59). For the W–E triple bond in the pnictido complexes [$(N_3N)W{\equiv}E$] (2.38, 2.35, 2.28 and 2.27 for E = P, As, Sb and Bi, respectively)[13] and [$(MeO)_3W{\equiv}E$] (2.56, 2.55, 2.54 and 2.54 for E = P, As, Sb and Bi, respectively) higher WBI were reported.[22]

Table 3. Wiberg bond indices for the W–E and E–Q bonds in complexes [$(N_3N)W(EQ)$] (**1**–**4**).

	E	W–E	E–Q	W–Q
		Q = O		
1a	P	1.83	1.34	0.30
2a	As	1.80	1.30	0.30
3a	Sb	1.70	1.20	0.28
4a	Bi	1.61	1.17	0.30
		Q = S		
1b	P	1.79	1.54	0.41
2b	As	1.79	1.49	0.39
3b	Sb	1.70	1.43	0.35
4b	Bi	1.62	1.39	0.35
		Q = Se		
1c	P	1.81	1.52	0.43
2c	As	1.79	1.48	0.41
3c	Sb	1.67	1.44	0.37
4c	Bi	1.59	1.41	0.37
		Q = Te		
1d	P	1.81	1.44	0.43
2d	As	1.79	1.43	0.41
3d	Sb	1.73	1.42	0.38
4d	Bi	1.64	1.42	0.38

In general, the W–E WBI decreases as the atomic number of E increases for a particular Q. The W–E WBI is not influenced by the nature of Q for a particular E and remains constant in the series. Also, the E–Q WIB decreases as the atomic number of E increases for a particular Q, but for the series **b**, **c** and **d** it is lower in magnitude then the decrease of the W–E WBI. For a particular E by moving from S to Te only a slight decrease of the E–Q WIB is observed. The WBI for the pnicogen monoxide complexes (**a**) are ca. 0.2 lower than for the other EQ complexes (**b**, **c**

and **d**). This is probably due to the higher ionicity of the pnicogen monoxide complexes.

To evaluate the ionic character of the complexes **1**–**4** we have analysed the Hirshfeld charge distribution (Table 4).[23,24] This shows that the equatorial nitrogen atoms of the amido (N_3N) ligands are negatively charged (–0.23), whereas the axial nitrogen atom is almost neutral (varies between 0 to –0.01) and both are not influenced by the nature of the EQ ligand. The positive charge on the tungsten atom is only slightly influenced by the nature of the EQ ligand (it varies between 0.33 and 0.40). As the atomic number of Q increases for a particular E the charge on the tungsten atom increases but it decreases as the atomic number of E increases for a particular Q (Figure 15). The charges on the pnicogen atom (E) vary between 0 and 0.34 for the PTe and BiO complexes, respectively (**1d** and **4a**, respectively), indicating a relatively strong variation (Table 4). Similarly, the negative charge on the chalcogen atoms also varies relatively strongly between the two extremes –0.12 and –0.44 for **1d** and **4a**, respectively. Generally, for a particular E the charges on either E and Q decrease as Q become heavier, while for a particular Q the charges on either E and Q increase as E becomes heavier (Figure 16). The Hirshfeld charge analysis shows that the complexes **b**–**d** are only moderately charged, while the pnicogen monoxide complexes (**a**) are more polar.

Table 4. Selected Hirshfeld charges in complexes [(N_3N)W(EQ)] (**1**–**4**).

	E	W	E	Q
		Q = O		
1a	P	0.36	0.17	–0.31
2a	As	0.36	0.21	–0.35
3a	Sb	0.33	0.32	–0.42
4a	Bi	0.33	0.34	–0.44
		Q = S		
1b	P	0.38	0.05	–0.18
2b	As	0.38	0.10	–0.22
3b	Sb	0.35	0.22	–0.30
4b	Bi	0.34	0.25	–0.32
		Q = Se		
1c	P	0.39	0.03	–0.15
2c	As	0.39	0.08	–0.20
3c	Sb	0.35	0.19	–0.27
4c	Bi	0.34	0.22	–0.30
		Q = Te		
1d	P	0.40	0.00	–0.12
2d	As	0.39	0.04	–0.16
3d	Sb	0.36	0.15	–0.22
4d	Bi	0.35	0.18	–0.25

One might expect that the decrease of the W–E bond strength (BDEs in Table 1) would be accompanied by an increase of the W–E distance. However, in the complexes **1**–**4** the W–E distances are shorter (except for **1d**) than in the pnictido complexes [(N_3N)W≡E], although the W–E BDEs are lower. This can be explained by the different hybridisation of the pnicogens in the two types of complexes. In the complexes **1**–**4** the pnicogen atom in the σ bonding is almost sp-hybridised ($sp^{0.5–0.7}$), while in the pnictido complexes it is $sp^{3.30}$- (E = P) to $sp^{6.06}$-hybridised (E = Bi).[13]

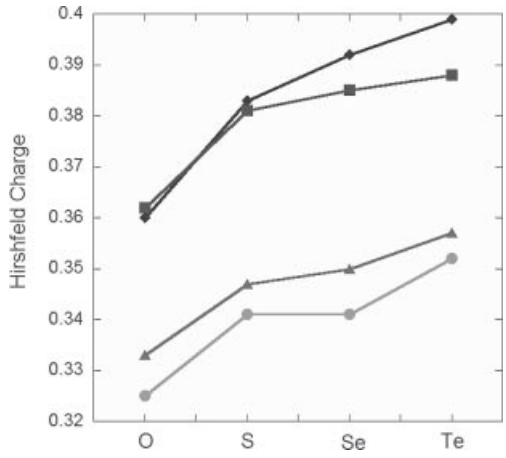

Figure 15. Variation of the Hirshfeld charges on tungsten in complexes [(N_3N)W(EQ)] (**1**–**4**). Legend: P = ♦, As = ■, Sb = ▲ and Bi = ●.

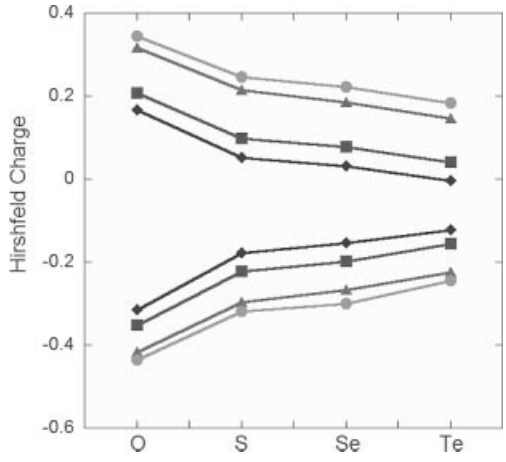

Figure 16. Variation of the Hirshfeld charges on E (positive) and Q (negative) in complexes [(N_3N)W(EQ)] (**1**–**4**). Legend: P = ♦, As = ■, Sb = ▲ and Bi = ●.

Since the s orbitals are more compact compared with the more diffuse p orbitals it is not unexpected that the effective radius of the pnicogen decreases with increase of the s contribution to the hybrid orbital through which the W–E σ bonding is realised. This decrease of the effective radius of E due to hybridisation is responsible for the shorter W–E bond in complexes **1**–**4** than in the corresponding pnictido [(N_3N)W≡E] complexes. Since the s-orbital contraction is more accentuated for the heavy elements, the shortening of the W–E bond will be more pronounced for the heavier congeners of E. This is consistent with the results of our calculations. It has to be noted that for the π bonding the pnicogen atoms use almost pure p orbitals in complexes **1**–**4** and [(N_3N)W≡E].

Conclusions about the hybridisation of the pnicogen atom in the phosphido complex [(N_3N)W≡P] was made based on ^{31}P NMR spectroscopy. The phosphido complex [(N_3N)W≡P] shows an unusual ^{31}P chemical shift (δ = 1080.0 ppm) and a small tungsten-phosphorus coupling constant ($^1J_{W-P}$ = 138 Hz).[10] The small tungsten-phospho-

rus coupling in the phosphido complex [(N_3N)W≡P] was attributed to the low s-orbital contribution to the W–P σ bonding[25] while the chemical shift was attributed to the paramagnetic shilding perpendicular to the W≡P triple bond.[26] In contrast to that, the phosphorus monosulfide complex **1b** presents a large phosphorus-tungsten coupling ($^1J_{W\text{-}P}$ = 771.5 Hz),[16] indicating a considerably higher amount of s-orbital contribution to the W–P σ bonding. We have calculated the ^{31}P chemical shift (δ = 356.8 ppm) and tungsten-phosphorus coupling ($^1J_{W\text{-}P}$ = 753.9 Hz) for **1b** which compare well with the experimental data (δ = 342.3 ppm, $^1J_{W\text{-}P}$ = 771.5 Hz). The NMR data and its predictibilty by computational procedures provides good evidence for the inferred cause of this unusual anti-correlation between bond strength and bond length.

Throughout chemistry there is a general correlation between bond length and bond strength, i.e. shorter bonds are stronger than longer bonds. However, there are exceptions. There are known examples where the bond lengths do not correlate with the bond strengths or force constants. For example in the H_nNF_{3-n} or Me_nNF_{3-n} series the N–F force constants increase with increasing bond length.[27] Also, for some polyfluorinated hydrocarbons an increase of the C–C dissociation energy with the bond length and increasing fluorine substitution was observed.[28] Distances were analysed computationally by Kaupp et al. with respect to their bond length/bond strength abnormality.[29] It was found that the Sn–Sn bond dissociation energy decreases clearly with increasing fluorine substitution but the Sn–Sn distance remains constant. Also, no correlation between the bond lengths and force constants was observed. This abnormality was attributed to "hybridisation-deficiency"[30] caused by "hybridisation defects" (reduced mixing and non-uniformity of the s and p orbitals due to their different radial distributions).[31] This work provides evidence that similar effects, i.e. hybridisation defects, cause the shortening of the W–E bond in complexes **1**–**4** compared to the pnictido complexes [(N_3N)W≡E].

Conclusions

In this paper we have shown, that the linear arrangement of the N_{ax}–W–E–Q framework in complexes of the type [(N_3N)W(EQ)] renders a bonding situation with a π-delocalised electron system which is best described as two three-centred four-electron bonds. The σ-electron systems becomes more localised as the atomic number of either E or Q increases. In contrast to the σ-electron system the π bonding becomes more delocalised as the atomic number of either E and Q increases. The strength of the *trans* influence of the EQ ligands in the complexes **1**–**4** is determined by the relative energy of the EQ fragment σ orbitals.

The shorter W–E distances in complexes **1**–**4** than in the pnictido complexes [(N_3N)W≡E] (E = P, As, Sb and Bi) have been attributed to the different hybridisation, i.e. considerable increase of s contribution to the σ MOs of the pnicogen atoms in complexes **1**–**4** compared to the pnictido [(N_3N)W≡E] complexes. Complexes **1**–**4** are moderately charged, except for the phosphorus monoxide complexes (**a**) which exhibit a more significant ionic character.

The W–E and E–Q bond dissociation energies of complexes **1**–**4** are relatively high, and show the expected periodic variations. The BDEs indicate that even the heavier congeners should be stable enough to be isolated. Both fragment calculations and WIB give very similar bond orders and trends herein. Overall, the bonding in the W–E–Q unit is best pictorially represented by two double bonds (Scheme 2).

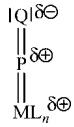

Scheme 2. Proposed Lewis structure for the complexes [(N_3N)-W(EQ)].

Computational Methods

DFT calculations were carried out using the Amsterdam Density Functional program (ADF) versions 2004.01 and 2005.01.[32–35] Scalar relativistic corrections were included via the Zero Order Regular Approximation (ZORA) method.[36–40] The generalized gradient approximation was employed, using the local density approximation of Vosko, Wilk, and Nusair[41] together with the nonlocal exchange correction by Becke[42,43] and nonlocal correlation corrections by Perdew.[44] The Slater-type orbital (STO) basis sets were of triple-ζ quality augmented with a single polarization function and two diffuse functions (ADF basis TZP++). The cores of the atoms were frozen up to 1s for C and N, 2p for P, S and Si, 3p for As and Se, 4p for Sb and Te, 5p for Bi and 4d for W. Optimisations were performed without symmetry restraints. Fragment calculations were performed to enable analysis of the orbital interactions to the W–E and E–Q bonds. In these calculations the complex is divided into two fragments, whose molecular and electronic structures are calculated in a single-point optimisation with a restricted singlet spin state. The geometry of the fragment is preserved from the optimised structure of the full complex. The molecular orbitals (MOs) of the complex are formed through linear combination of the MOs of the two fragments. The bond dissociation energies (BDEs) were calculated as the difference between the energy of the complex and the energy of the fragments in their ground state [Q triplet, (N_3N)WE singlet, EQ doublet and (N_3N)W quartet]. For the BDEs the SCF energies were used without correction. The ^{31}P NMR chemical shift and P–W coupling constant for **1b** were calculated on the optimised geometry using the corresponding program modules as implemented in ADF.[45–49] The geometry of **1b** was optimised with the TZ2P basis sets for all atoms, with no core electrons and using a tight convergence criterion as well as an integration grid of 6. The relativistic effects were incorporated via the ZORA method. NBO analyses were performed with the Gaussian03 program[50] using the BP86[42–44] functional and the 6-31G* basis sets[51–59] with one diffuse function added, for C, H, N, Si, P, S, As and Se. The Dunning–Hunzinaga[60] type basis set with Stuttgart–Dresden SDD[61,62] core potentials was applied for Sb, Te, W and Bi.

Supporting Information (see footnote on the first page of this article): Tables of the fragment analyses and cartesian coordinates for all optimised structures. Figures in colour are also included.

Acknowledgments

G. B. thanks the von Humboldt Foundation for a Feodor Lynen fellowship. The Oxford Supercomputing Centre is acknowledged for the computing facilities.

[1] J. E. Huheey, E. A. Kreiter, R. L. Kreiter, *Inorganic Chemistry: Principles of Structure and Reactivity*, 4th ed., Addison-Wesley, New York, **1993**.
[2] A. Holleman, E. Wiberg, *Lehrbuch der Anorganischen Chemie*, de Gruyter, Berlin, **1995**.
[3] O. J. Scherer, J. Braun, P. Walther, G. Heckmann, G. Wolmershaeuser, *Angew. Chem.* **1991**, *103*, 861.
[4] J. F. Corrigan, S. Doherty, N. J. Taylor, A. J. Carty, *J. Am. Chem. Soc.* **1994**, *116*, 9799.
[5] J. E. Davies, M. J. Mays, E. J. Pook, P. R. Raithby, P. K. Tompkin, *Chem. Commun.* **1997**, 1997.
[6] O. J. Scherer, S. Weigel, G. Wolmershauser, *Heteroat. Chem.* **1999**, *10*, 622.
[7] O. J. Scherer, C. Vondung, G. Wolmershauser, *Angew. Chem. Int. Ed. Engl.* **1997**, *36*, 1303.
[8] I.-P. Lorenz, W. Pohl, K. Polborn, *Chem. Ber.* **1996**, *129*, 11.
[9] C. E. Laplaza, W. M. Davis, C. C. Cummins, *Angew. Chem. Int. Ed. Engl.* **1995**, *34*, 2042.
[10] N. C. Zanetti, R. R. Schrock, W. M. Davis, *Angew. Chem. Int. Ed. Engl.* **1995**, *34*, 2044.
[11] N. C. Moesch-Zanetti, R. R. Schrock, W. M. Davis, K. Wanninger, S. W. Seidel, M. B. O'Donoghue, *J. Am. Chem. Soc.* **1997**, *119*, 11037.
[12] M. Scheer, J. Müller, M. Häser, *Angew. Chem. Int. Ed. Engl.* **1996**, *35*, 2492.
[13] G. Balázs, M. Sierka, M. Scheer, *Angew. Chem. Int. Ed.* **2005**, *44*, 4920.
[14] M. J. A. Johnson, A. L. Odom, C. C. Cummins, *Chem. Commun.* **1997**, 1523.
[15] C. C. Cummins, *Chem. Commun.* **1998**, 1777.
[16] G. Balázs, J. C. Green, M. Scheer, *Chem. Eur. J.* **2006**, *12*, 8603.
[17] T. Wagener, G. Frenking, *Inorg. Chem.* **1998**, *37*, 6402.
[18] T. Wagener, G. Frenking, *Inorg. Chem.* **1998**, *37*, 1805.
[19] P. Pyykkö, S. Riedel, M. Patzschke, *Chem. Eur. J.* **2005**, *11*, 3511.
[20] A. Bérces, O. Koentjoro, B. T. Sterenberg, J. H. Yamamoto, J. Tse, A. J. Carty, *Organometallics* **2000**, *19*, 4336.
[21] K. B. Wiberg, *Tetrahedron* **1968**, *24*, 1083.
[22] K. K. Pandey, G. Frenking, *Eur. J. Inorg. Chem.* **2004**, 4388.
[23] K. B. Wiberg, P. R. Rablen, *J. Comput. Chem.* **1993**, *14*, 1504.
[24] F. L. Hirshfeld, *Theor. Chim. Acta* **1977**, *44*, 129.
[25] J. A. Johnson-Carr, N. C. Zanetti, R. R. Schrock, M. D. Hopkins, *J. Am. Chem. Soc.* **1996**, *118*, 11305.
[26] G. Wu, D. Rovnyak, M. J. A. Johnson, N. C. Zanetti, D. G. Musaev, K. Morokuma, R. R. Schrock, R. G. Griffin, C. C. Cummins, *J. Am. Chem. Soc.* **1996**, *118*, 10654.
[27] D. Christen, O. D. Gupta, J. Kadel, R. L. Kirchmeier, H. G. Mack, H. Oberhammer, J. M. Shreeve, *J. Am. Chem. Soc.* **1991**, *113*, 9131.
[28] B. E. Smart, in *Molecular Structures and Energetics*, vol. 3 (Eds.: J. F. Liebmann, A. Greenberg), Verlag Chemie, Weinheim, **1968**, p. 141.
[29] M. Kaupp, B. Metz, H. Stoll, *Angew. Chem. Int. Ed.* **2000**, *39*, 4607.
[30] W. Kutzelnigg, *Angew. Chem.* **1984**, *96*, 262.
[31] M. Kaupp, P. v. R. Schleyer, *J. Am. Chem. Soc.* **1993**, *115*, 1061.
[32] G. Te Velde, F. M. Bickelhaupt, E. J. Baerends, C. Fonseca Guerra, S. J. A. Van Gisbergen, J. G. Snijders, T. Ziegler, *J. Comput. Chem.* **2001**, *22*, 931.
[33] C. Fonseca Guerra, J. G. Snijder, G. Te Velde, E. J. Baerends, *Theor. Chem. Acc.* **1998**, *99*, 391.
[34] In ADF2004.01, SCM, Theoretical Chemistry, Vrije Universiteit, Amsterdam, The Netherlands, http://www.scm.com.
[35] In ADF2002.02, SCM, Theoretical Chemistry, Vrije Universiteit, Amsterdam, The Netherlands, http://www.scm.com.
[36] E. van Lenthe, A. Ehlers, E. J. Baerends, *J. Chem. Phys.* **1999**, *110*, 8943.
[37] E. van Lenthe, R. van Leeuwen, E. J. Baerends, J. G. Snijders, *Int. J. Quantum Chem.* **1996**, *57*, 281.
[38] E. van Lenthe, E. J. Baerends, J. G. Snijders, *J. Chem. Phys.* **1996**, *105*, 6505.
[39] E. van Lenthe, E. J. Baerends, J. G. Snijders, *J. Chem. Phys.* **1994**, *101*, 9783.
[40] E. van Lenthe, E. J. Baerends, J. G. Snijders, *J. Chem. Phys.* **1993**, *99*, 4597.
[41] S. H. Vosko, L. Wilk, M. Nusair, *Can. J. Phys.* **1980**, *58*, 1200.
[42] A. D. Becke, *J. Chem. Phys.* **1988**, *88*, 1053.
[43] A. D. Becke, *Phys. Rev. A* **1988**, *38*, 3098.
[44] J. P. Perdew, *Phys. Rev. B* **1986**, *33*, 8800.
[45] J. Autschbach, T. Ziegler, *J. Chem. Phys.* **2000**, *113*, 936.
[46] J. Autschbach, T. Ziegler, *J. Chem. Phys.* **2000**, *113*, 9410.
[47] G. Schreckenbach, T. Ziegler, *J. Phys. Chem.* **1995**, *99*, 606.
[48] G. Schreckenbach, T. Ziegler, *Int. J. Quantum Chem.* **1997**, *61*, 899.
[49] S. K. Wolff, T. Ziegler, *J. Chem. Phys.* **1998**, *109*, 895.
[50] M. J. Frisch, G. W. Trucks, H. B. Schlegel, G. E. Scuseria, M. A. Robb, J. R. Cheeseman, J. A. Montgomery, T. Vreven, K. N. Kudin, J. C. Burant, J. M. Millam, S. S. Iyengar, J. Tomasi, V. Barone, B. Mennucci, M. Cossi, G. Scalmani, N. Rega, G. A. Petersson, H. Nakatsuji, M. Hada, M. Ehara, K. Toyota, R. Fukuda, J. Hasegawa, M. Ishida, T. Nakajima, Y. Honda, O. Kitao, H. Nakai, M. Klene, X. Li, J. E. Knox, H. P. Hratchian, J. B. Cross, V. Bakken, C. Adamo, J. Jaramillo, R. Gomperts, R. E. Stratmann, O. Yazyev, A. J. Austin, R. Cammi, C. Pomelli, J. W. Ochterski, P. Y. Ayala, K. Morokuma, G. A. Voth, P. Salvador, J. J. Dannenberg, V. G. Zakrzewski, S. Dapprich, A. D. Daniels, M. C. Strain, O. Farkas, D. K. Malick, A. D. Rabuck, K. Raghavachari, J. B. Foresman, J. V. Ortiz, Q. Cui, A. G. Baboul, S. Clifford, J. Cioslowski, B. B. Stefanov, G. Liu, A. Liashenko, P. Piskorz, I. Komaromi, R. L. Martin, D. J. Fox, T. Keith, M. A. Al-Laham, C. Y. Peng, A. Nanayakkara, M. Challacombe, P. M. W. Gill, B. Johnson, W. Chen, M. W. Wong, C. Gonzalez, J. A. Pople, *Gaussian03*, Gaussian Inc., Wallingford CT, **2004**.
[51] R. Ditchfield, W. J. Hehre, J. A. Pople, *J. Chem. Phys.* **1971**, *54*, 724.
[52] W. J. Hehre, R. Ditchfield, J. A. Pople, *J. Chem. Phys.* **1972**, *56*, 2257.
[53] P. C. Hariharan, J. A. Pople, *Theor. Chim. Acta* **1973**, *28*, 213.
[54] P. C. Hariharan, J. A. Pople, *Mol. Phys.* **1974**, *27*, 209.
[55] M. M. Francl, W. J. Pietro, W. J. Hehre, J. S. Binkley, D. J. DeFrees, J. A. Pople, M. S. Gordon, *J. Chem. Phys.* **1982**, *77*, 3654.
[56] R. C. J. Binning, L. A. Curtiss, *J. Comput. Chem.* **1990**, *11*, 1206.
[57] J.-P. Blaudeau, M. P. McGrath, L. A. Curtiss, L. Radom, *J. Chem. Phys.* **1997**, *107*, 5016.
[58] V. A. Rassolov, J. A. Pople, M. A. Ratner, T. L. Windus, *J. Chem. Phys.* **1998**, *109*, 1223.
[59] V. A. Rassolov, M. A. Ratner, J. A. Pople, P. C. Redfern, L. A. Curtiss, *J. Comput. Chem.* **2001**, *22*, 976.
[60] T. H. Dunning, P. J. Hay, in *Modern Theoretical Chemistry*, vol. 3 (Ed.: H. F. Schaefer), Plenum, New York, **1976**, p. 1.
[61] M. Dolg, U. Wedig, H. Stoll, H. Preuss, *J. Chem. Phys.* **1987**, *86*, 866.
[62] A. Bergner, M. Dolg, W. Kuechle, H. Stoll, H. Preuss, *Mol. Phys.* **1993**, *80*, 1431.

Received: January 12, 2007
Published Online: April 30, 2007

